Weierstraß-Institut

für Angewandte Analysis und Stochastik

Leibniz-Institut im Forschungsverbund Berlin e. V.

Preprint ISSN 0946 – 8633

An optimization method in inverse elastic scattering for one-dimensional grating profiles

Johannes Elschner, Guanghui Hu

submitted: June 22, 2011

Weierstrass Institute
Mohrenstr. 39
10117 Berlin
Germany
E-Mail: johannes.elschner@wias-berlin.de
guanghui.hu@wias-berlin.de

No. 1622
Berlin 2011

2010 *Mathematics Subject Classification.* 35R30, 74B05, 78A46, 35Q93.

Key words and phrases. Diffraction grating, elastic waves, profile reconstruction, Tikhonov regularization, optimization method.

The second author gratefully acknowledges the support by the German Research Foundation (DFG) under Grant No. EL 584/1-2.

Edited by
Weierstraß-Institut für Angewandte Analysis und Stochastik (WIAS)
Leibniz-Institut im Forschungsverbund Berlin e. V.
Mohrenstraße 39
10117 Berlin
Germany

Fax: +49 30 2044975
E-Mail: preprint@wias-berlin.de
World Wide Web: http://www.wias-berlin.de/

Abstract

Consider the inverse diffraction problem to determine a two-dimensional periodic structure from scattered elastic waves measured above the structure. We formulate the inverse problem as a least squares optimization problem, following the two-step algorithm by G. Bruckner and J. Elschner (2003 *Inverse Problems* **19** 315-329) for electromagnetic diffraction gratings. Such a method is based on the Kirsch-Kress optimization scheme and consists of two parts: a linear severely ill-posed problem and a nonlinear well-posed one. We apply this method to both smooth (C^2) and piecewise linear gratings for the Dirichlet boundary value problem of the Navier equation. Numerical reconstructions from exact and noisy data illustrate the feasibility of the method.

1 Introduction

The inverse scattering problem of recovering an unknown grating profile from the scattered field is of great importance, e.g., in quality control and design of diffractive elements with prescribed far-field patterns [8, 25]. This paper is concerned with the two-dimensional inverse elastic scattering problem for a 2π-periodic structure under the Dirichlet boundary condition, i.e., the total displacement vanishes on the scattering surface.

Existence and uniqueness results on the forward problem of elastic scattering are obtained in [2, 13, 15], while the uniqueness to the inverse problem is studied in [1] for the Dirichlet problem and in [14, 16] for the third and fourth kind boundary conditions. As far as we know, there does not exist any reference dealing with the inversion algorithm of determining a grating profile from scattered elastic waves for the Navier equation. The purpose of this paper is to fill this gap by extending the two-step algorithm proposed by G. Bruckner and J. Elschner in [9] to elastic scattering problems.

There is already a vast literature on the reconstruction of a perfectly conducting profile for the two-dimensional Helmholtz equation. Here we mention a conjugate gradient algorithm based on analytic continuation [21], an iterative regularization method [19], the Kirsch-Kress optimization algorithm [9, 10, 11] and the factorization method of Kirsch [5, 6]. Based on the Kirsch-Kress scheme (see [12, Chapter 5] and the references therein), a two-step algorithm for reconstructing the grating profile is proposed in [9]. The first step is to reconstruct the scattered field from near-field measurements by solving a first kind integral equation. This step is the linear severely ill-posed part and requires the Tikhonov regularization where the singular value decomposition of the integral operator is involved. The second step is to approximate the inverse solution by solving a finite dimensional least squares problem, which is non-linear but well-posed. The advantages of the two-step algorithm are the following. (i) It reduces the computational effort for the Kirsch-Kress scheme which is based on a combined cost functional that requires the determination of two unknown functions. This is mainly because the singular value decomposition of the derived first kind integral equation can be readily achieved, and only the unknown grating profile

function needs to be determined in the second step. (ii) One does not need to solve direct scattering problems in the process of the inversion algorithm. Note that so far the uniqueness in the inverse problem is not known for general grating profiles, and we have no convergence results for the two-step algorithm. We refer to the convergence analysis in [18] for the Kirsch-Kress optimization method applied to the 2D quasi-periodic Helmholtz equation and the reconstruction of general Lipschitz grating profiles. We think that these convergence results can be extended to the elastic case.

In this paper we always assume that the incident elastic wave is an incoming pressure wave, and our method can be easily extended to the case of an incident shear wave. We present numerical results for C^2-smooth and piecewise linear gratings, including the binary gratings. Note that a binary grating profile is composed of only a finite number of horizontal and vertical line segments and has many practical applications in the design of complicated grating structures. The numerical reconstruction from far-field data for several incoming pressure waves with different incident angles is also reported, which is more practical from the engineering point of view. Our numerical experiments for exact and noisy data demonstrate the efficiency and practicability of the inversion algorithm.

The paper is organized as follows. In the next section we rigorously formulate the direct and inverse elastic scattering problems for diffraction gratings. The quasi-periodic fundamental solution to the Navier equation is investigated in Section 3. In our numerical experiments we generate synthetic scattering data by solving a first kind integral equation and using the discrete Galerkin methods proposed in [7] for a smooth grating profile and that in [17] for a piecewise linear grating profile; see Section 4. A similar method is used in [22] for solving the forward problem of elastic scattering from an open arc in $\mathbb{R}^2$. The implementation of the reconstruction algorithm as a two-step method will be discussed in Section 5, and some numerical examples are reported in Section 6. In the final Section 7 we give some conclusions and remarks.

2 Direct and inverse diffraction problems

Consider the scattering of time-harmonic elastic waves by a two-dimensional impenetrable diffraction grating where the total displacement vanishes on the scattering surface. This can be modelled by the Dirichlet boundary value problem for the Navier equation in the unbounded domain above the grating profile.

Let the profile of the diffraction grating be given by a curve Λ which is 2π-periodic with respect to x_1. In this paper, we assume that Λ is the graph of a function f which is either C^2-smooth or piecewise linear. In the special case of a piecewise constant function f, Λ is called a binary grating, which only consists of a finite number of horizontal and vertical line segments. Denote the unbounded region above Λ by Ω_Λ, and for simplicity assume that Ω_Λ is filled with a linear isotropic and homogeneous elastic material whose mass density is equal to one. Suppose that an incident pressure wave (with the incident angle $\theta \in (-\pi/2, \pi/2)$) given by

$$u^{in} = \hat{\theta} \exp(ik_p x \cdot \hat{\theta}), \qquad \hat{\theta} := (\sin\theta, -\cos\theta)^T \tag{2.1}$$

is incident on Λ from Ω_Λ, where $k_p := \omega/\sqrt{2\mu+\lambda}$ is the compressional wave number, λ and μ denote the Lamé constants satisfying $\mu > 0$ and $\lambda + \mu > 0$, $\omega > 0$ denotes the angular frequency of the harmonic motion, and the symbol $(\cdot)^T$ stands for the transpose of a vector in $\mathbb{R}^2$. The shear wave number is defined as $k_s := \omega/\sqrt{\mu}$. The direct problem (**DP**) is to find the scattered field $u \in H^1_{loc}(\Omega_\Lambda)^2$ such

that

$$\begin{aligned}(\Delta^* + \omega^2)u &= 0 \quad \text{in} \quad \Omega_\Lambda\,, \quad \Delta^* := \mu\Delta + (\lambda+\mu)\,\mathrm{grad}\,\mathrm{div}\ , \\ u &= -u^{in} \quad \text{on} \quad \Lambda,\end{aligned} \tag{2.2}$$

where u is assumed to be quasiperiodic with the phase-shift $\alpha := k_p \sin\theta$ (or α-quasiperiodic):

$$u(x_1 + 2\pi, x_2) = \exp(2i\alpha\pi)\, u(x_1, x_2)\,, \quad (x_1, x_2) \in \Omega_\Lambda\,. \tag{2.3}$$

Moreover, the solution u is required to satisfy the Rayleigh expansion (or outgoing wave condition, see [2, 13]) :

$$u(x) = \sum_{n\in\mathbb{Z}} \left\{ A_{p,n} \begin{pmatrix} \alpha_n \\ \beta_n \end{pmatrix} \exp(i\alpha_n x_1 + i\beta_n x_2) + A_{s,n} \begin{pmatrix} \gamma_n \\ -\alpha_n \end{pmatrix} \exp(i\alpha_n x_1 + i\gamma_n x_2) \right\}, \tag{2.4}$$

for $x_2 > \Lambda^+ := \max_{(x_1,x_2)\in\Lambda} x_2$, where the constants $A_{p,n},\ A_{s,n} \in \mathbb{C}$ are called the Rayleigh coefficients. Moreover,

$$\alpha_n := \alpha + n\,, \quad \beta_n = \beta_n(\theta) := \begin{cases} \sqrt{k_p^2 - \alpha_n^2} & \text{if} \quad |\alpha_n| \le k_p \\ i\sqrt{\alpha_n^2 - k_p^2} & \text{if} \quad |\alpha_n| > k_p\,, \end{cases} \tag{2.5}$$

and $\gamma_n := \gamma_n(\theta)$ is defined analogously as β_n with k_p replaced by k_s. Since β_n and γ_n are real for at most a finite number of indices $n \in \mathbb{Z}$, only a finite number of plane waves in (2.4) propagate into the far field, with the remaining evanescent waves (or surface waves) decaying exponentially as $x_2 \to +\infty$. The above expansion converges uniformly with all derivatives in the half-plane $\{x \in \mathbb{R}^2 : x_2 \ge b\}$, for any $b > \Lambda^+$. Define the compressional part u_p and the shear part u_s of the Rayleigh expansion (2.4) as

$$\begin{aligned} u_p &:= \sum_{n\in\mathbb{Z}} A_{p,n}(\alpha_n, \beta_n)^T \exp(i\alpha_n x_1 + i\beta_n x_2), \quad x_2 > \Lambda^+, \\ u_s &:= \sum_{n\in\mathbb{Z}} A_{s,n}(\gamma_n, -\alpha_n)^T \exp(i\alpha_n x_1 + i\gamma_n x_2), \quad x_2 > \Lambda^+ \end{aligned}$$

respectively. We see that $u = u_p + u_s$ with u_p and u_s satisfying $\mathrm{curl}\, u_p = 0, \mathrm{div}\, u_s = 0$, where $\mathrm{curl}\, v := \partial_1 v_2 - \partial_2 v_1$ for $v = (v_1, v_2)^T$, and $(\Delta + k_p^2)u_p = 0, (\Delta + k_s^2)u_s = 0$.

The first attempt to rigorously prove existence and uniqueness of solutions to (**DP**) is due to T. Arens; see [2] where the boundary integral equation method is used provided the grating profile Λ is given by the graph of a smooth (C^2) periodic function. Using a variational method, it is shown in [13] that there always exists a quasi-periodic solution to (**DP**) by establishing the strong ellipticity of the corresponding variational formulation over a bounded periodic cell and then applying the Fredholm alternative. Moreover, uniqueness can be guaranteed if the grating profile is given by a Lipschitz graph (and also for binary grating profiles). For further solvability results we refer to [3, 4] in the case of rough surfaces in $\mathbb{R}^2$ and to [15] for elastic diffraction grating problems in $\mathbb{R}^3$.

Since the surface waves far away from the grating can be hardly measured, the inverse problem always involves near-field measurements $u(x_1, b)$ for some fixed $b > \Lambda^+$.

Inverse problem (IP): Determine the grating profile Λ from the knowledge of the near-field data $u(x_1, b; \theta)$ for all $x_1 \in (0, 2\pi)$. Here $u(x; \theta)$ is the unique solution of (DP) for the incident pressure wave $u^{in}(x)$ defined in (2.1) with the incident angle $\theta \in (-\frac{\pi}{2}, \frac{\pi}{2})$.

Note that the problem (IP) is nonlinear and severely ill-posed. Concerning uniqueness in (IP), it is proved in [1] that a smooth grating surface (C^2) can be uniquely determined from incident pressure waves for one incident angle and an interval of wave numbers. Furthermore, a finite set of wave numbers is enough if *a priori* information about the height of the grating curve is known, and in particular uniqueness with one incident wave holds for grating profiles with a small height. This extends the Hettlich and Kirsch work on Schiffer's theorem (see [20]) to the case of inverse elastic diffraction problems. Under the boundary conditions of the third or fourth kind (note that the Dirichlet boundary condition corresponds to the first kind boundary condition), one can determine and classify all the polygonal or polyhedral grating profiles that cannot be uniquely identified by one incident pressure wave, see [14, 16]. Unfortunately, the uniqueness results in ([14, 16]) do not cover our problem (IP) involving the Dirichlet boundary condition. Thus, we do not have uniqueness in (IP) for general grating profiles.

As mentioned earlier, only a finite number of propagating modes of the compressional and shear parts can be measured far away from the grating surface. Thus it is quite natural from the practical point of view to reconstruct the unknown grating profile from the far-field data $u_b^\infty(x_1)$ of $u(x)$ defined by

$$\begin{aligned} u_b^\infty(x_1) &= \sum_{n\in\mathcal{U}_p} A_{p,n}(\alpha_n,\beta_n)^T \exp(i\alpha_n x_1 + i\beta_n b) \\ &\quad + \sum_{n\in\mathcal{U}_s} A_{s,n}(\gamma_n,-\alpha_n)^T \exp(i\alpha_n x_1 + i\gamma_n b) \end{aligned}$$

for some $b > \Lambda^+$, where

$$\mathcal{U}_p = \{n\in\mathbb{Z} : |\alpha_n| \le k_p\}, \quad \mathcal{U}_s = \{n\in\mathbb{Z} : |\alpha_n| \le k_s\}.$$

Throughout the paper, we assume that $\beta_n \neq 0, \gamma_n \neq 0$ for all $n \in \mathbb{Z}$, i.e., the Rayleigh frequencies of the compressional and shear parts are both excluded. In this paper we also consider the following inverse problem:

Inverse problem (IP*): Determine the grating profile Λ from the knowledge of the far-field data $u_b^\infty(x_1;\theta_\tau)$ for all $x_1 \in (0,2\pi)$, $\tau = 1,2,\cdots,m$, where $u(x;\theta_\tau)$ denotes the unique solution of (DP) for the incident pressure wave $u^{in}(x)$ with the incident angle $\theta_\tau \in (-\frac{\pi}{2},\frac{\pi}{2})$.

We also report numerical results in the case of far-field data corresponding to one or several incoming pressure waves, where only the knowledge of the Rayleigh coefficients $A_{p,n}$ for $n \in \mathcal{U}_p$ and $A_{s,n}$ for $n \in \mathcal{U}_s$ is required.

3 Quasiperiodic fundamental solution to the Navier equation

In this section we review some properties of the quasiperiodic Green tensor to the Navier equation (2.2). We first recall the free space fundamental solution to the Helmholtz equation $(\Delta + k^2)u = 0$ given by

$$\Phi_k(x,y) = \frac{i}{4}H_0^{(1)}(k|x-y|), \quad x \neq y,\ x=(x_1,x_2), y=(y_1,y_2) \in \mathbb{R}^2,$$

with $H_0^{(1)}(t)$ being the first kind Hankel function of order zero, and then recall the α-quasiperiodic fundamental solution to the Helmholtz equation $(\Delta + k^2)u = 0$ defined by (see e.g. [23])

$$\begin{aligned} G_k(x,y) &= \sum_{n\in\mathbb{Z}} \exp(-i\alpha 2\pi n)\Phi_k(x+n(2\pi,0),y) \\ &= \frac{i}{4\pi}\sum_{n\in\mathbb{Z}}\frac{1}{\beta_n}\exp(i\alpha_n(x_1-y_1)+i\beta_n|x_2-y_2|), \end{aligned}$$

for $x - y \neq n(2\pi, 0)$, $n \in \mathbb{Z}$, where β_n are defined as in (2.5) with k_p replaced by k. The fundamental solution to the Navier equation (2.2) is given by (see e.g. [22])

$$\begin{aligned} \Gamma(x,y) &= \frac{i}{4\mu}H_0^{(1)}(k_s|x-y|)\ I + \frac{i}{4\omega^2}\mathrm{grad}_x\mathrm{grad}_x^T\left[H_0^{(1)}(k_s|x-y|) - H_0^{(1)}(k_p|x-y|)\right] \\ &= \frac{1}{\mu}\Phi_{k_s}(x,y)\ I + \frac{1}{\omega^2}\mathrm{grad}_x\mathrm{grad}_x^T\left[\Phi_{k_s}(x,y) - \Phi_{k_p}(x,y)\right], \end{aligned}$$

where I stands for the 2×2 unit matrix. Then, the α-quasiperiodic fundamental solution (Green's tensor) to the Navier equation (2.2) takes the form

$$\begin{aligned} \Pi(x,y) &:= \sum_{n\in\mathbb{Z}}\exp(-i\alpha 2\pi n)\Gamma(x+n(2\pi,0),y) \\ &= \Gamma(x,y) + \sum_{|n|\geq 1}\exp(-i\alpha 2\pi n)\Gamma(x+n(2\pi,0),y) \end{aligned}$$

for $x-y \neq n(2\pi,0), n\in\mathbb{Z}$. The convergence of the above series for $\Pi(x,y)$ is discussed in [2, Section 6]. In view of the representations of $G_k(x,y)$ and $\Gamma(x,y)$, we can rewrite $\Pi(x,y)$ as

$$\begin{aligned} \Pi(x,y) &= \frac{1}{\mu}G_{k_s}(x,y)I + \frac{1}{\omega^2}\mathrm{grad}_x\mathrm{grad}_x^T\left[G_{k_s}(x,y) - G_{k_p}(x,y)\right] \\ &= \frac{1}{\mu}\begin{pmatrix} G_{k_s}(x,y) & 0 \\ 0 & G_{k_s}(x,y)\end{pmatrix} + \frac{1}{\omega^2}\begin{pmatrix}\partial_{x_1}^2 & \partial_{x_1}\partial_{x_2}\\ \partial_{x_2}\partial_{x_1} & \partial_{x_2}^2\end{pmatrix}\left[G_{k_s}(x,y) - G_{k_p}(x,y)\right] \end{aligned} \quad (3.6)$$

Recall [22] that $\Gamma(x,y)$ can be decomposed as

$$\Gamma(x,y) = \frac{1}{\pi}\ln(|x-y|)\Gamma_1(x,y) + \Gamma_2(x,y),$$

with

$$\begin{aligned} \Gamma_1(x,y) &= \Psi_1(|x-y|)\ I + \Psi_2(|x-y|)\ \Xi(x,y), \\ \Gamma_2(x,y) &:= \Gamma(x,y) - \tfrac{1}{\pi}\ln(|x-y|)\Gamma_1(x,y) = \chi_1(|x-y|)\ I + \chi_2(|x-y|)\ \Xi(x,y), \end{aligned}$$

where $\chi_j(\tau)$ $(j=1,2)$ are C^∞ functions on $\mathbb{R}^+$, and

$$\begin{aligned} \Xi(x,y) &= \frac{1}{|x-y|^2}\begin{pmatrix}(x_1-y_1)^2 & (x_1-y_1)(x_2-y_2)\\ (x_1-y_1)(x_2-y_2) & (x_2-y_2)^2\end{pmatrix}, \\ \Psi_1(\tau) &= -\frac{1}{2\mu}J_0(k_s\tau) + \frac{1}{2\omega^2\tau}(k_sJ_1(k_s\tau) - k_pJ_1(k_p\tau)), \\ \Psi_2(\tau) &= \frac{1}{2\omega^2}\left[k_s^2J_0(k_s\tau) - \frac{2k_s}{\tau}J_1(k_s\tau) - k_p^2J_0(k_p\tau) + \frac{2k_p}{\tau}J_1(k_p\tau)\right], \end{aligned}$$

with the Bessel functions $J_0(t)$ and $J_1(t)$. Furthermore, making use of the asymptotic behavior

$$J_0(t) = 1 - \frac{1}{4}t^2 + \frac{1}{64}t^4 + \mathcal{O}(t^6), \quad J_1(t) = \frac{1}{2}t - \frac{1}{16}t^3 + \mathcal{O}(t^5), \quad t \to 0^+$$

we see that (see also [22])

$$\begin{aligned}
&\Psi_1(\tau) = -\eta_1 + \eta_2\,\tau^2 + \mathcal{O}(\tau^4), \quad \Psi_2(\tau) = \eta_3\,\tau^2 + \mathcal{O}(\tau^4),\\
&\chi_1(\tau) = \eta_4 + \mathcal{O}(\tau^2), \quad \chi_2(\tau) = \eta_5 + (\tau^2)
\end{aligned}$$

as $\tau \to 0$, where

$$\begin{aligned}
&\eta_1 = \frac{1}{4\omega^2}(k_s^2 + k_p^2),\ \eta_2 = \frac{1}{32\omega^2}(3k_s^4 + k_p^4),\ \eta_3 = \frac{1}{16\omega^2}(k_p^4 - k_s^4),\\
&\eta_4 = -\frac{1}{4\pi\omega^2}\left[k_s^2 \ln\frac{k_s}{2} + k_p^2 \ln\frac{k_p}{2} + \frac{k_s^2 - k_p^2}{2} + (C - \frac{i\pi}{2})(k_s^2 + k_p^2)\right],\ \eta_5 = \frac{k_s^2 - k_p^2}{4\pi\omega^2},
\end{aligned}$$

with Euler's constant $C = 0.57721\cdots$. Now we can see that both $\Gamma(x,y)$ and $\Pi(x,y)$ have a logarithmic singularity of the form

$$\Gamma(x,y) = -\eta_1\frac{1}{\pi}\ln(|x-y|)\,I + \Gamma^*(x,y), \quad \Pi(x,y) = -\eta_1\frac{1}{\pi}\ln(|x-y|)\,I + \Pi^*(x,y), \tag{3.7}$$

where

$$\begin{aligned}
\Gamma^*(x,y) &:= \Gamma(x,y) + \eta_1\frac{1}{\pi}\ln(|x-y|)\,I,\\
&= \frac{1}{\pi}\ln(|x-y|)\,[(\Psi_1(|x-y|) + \eta_1)\,I + \Psi_2(|x-y|)\,\Xi(x,y)\,]\\
&\quad +\chi_1(|x-y|)\,I + \chi_2(|x-y|)\,\Xi(x,y),\\
\Pi^*(x,y) &:= \Pi(x,y) + \eta_1\frac{1}{\pi}\ln(|x-y|)\,I\\
&= \Gamma^*(|x-y|) + \sum_{|n|\geq 1}\exp(-i\alpha 2\pi n)\Gamma(x + n(2\pi,0), y)
\end{aligned}$$

are both continuously differentiable matrices in the variables x, y on the C^2-smooth grating profile Λ. The decomposition (3.7) will be used in Section 4 to generate synthetic scattering data by solving a first kind integral equation.

Finally, we derive from (3.6) and the definitions of $G_k(x,y)$ that

$$\Pi(x,y) = \begin{pmatrix}\Pi_{11} & \Pi_{12}\\ \Pi_{21} & \Pi_{22}\end{pmatrix},$$

with

$$\Pi_{ij} = \sum_{n\in\mathbb{Z}} P_{ij}^{(n)}\exp(i[\alpha_n(x_1 - y_1) + \beta_n|x_2 - y_2|]) + S_{ij}^{(n)}\exp(i[\alpha_n(x_1 - y_1) + \gamma_n|x_2 - y_2|]),$$

where, for $x_2 > y_2$, the constants $P_{ij}^{(n)}, S_{ij}^{(n)} \in \mathbb{C}$ for $1 \leq i,j \leq 2, n \in \mathbb{Z}$ are given by

$$\begin{pmatrix}P_{11}^{(n)} & P_{12}^{(n)}\\ P_{21}^{(n)} & P_{22}^{(n)}\end{pmatrix} = \frac{1}{4\pi\omega^2\beta_n}\begin{pmatrix}\alpha_n^2 & \alpha_n\beta_n\\ \alpha_n\beta_n & \beta_n^2\end{pmatrix} =: P^{(n)}, \tag{3.8}$$

$$\begin{pmatrix}S_{11}^{(n)} & S_{12}^{(n)}\\ S_{21}^{(n)} & S_{22}^{(n)}\end{pmatrix} = \frac{i}{4\pi\mu\gamma_n}\,I - \frac{1}{4\pi\omega^2\gamma_n}\begin{pmatrix}\alpha_n^2 & \alpha_n\gamma_n\\ \alpha_n\gamma_n & \gamma_n^2\end{pmatrix} =: S^{(n)}. \tag{3.9}$$

This enables us to rewrite $\Pi(x,y)$ in the form

$$\Pi(x,y) = \sum_{n\in\mathbb{Z}} P^{(n)} \exp(i[\alpha_n(x_1-y_1)+\beta_n|x_2-y_2|]) + \sum_{n\in\mathbb{Z}} S^{(n)} \exp(i[\alpha_n(x_1-y_1)+\gamma_n|x_2-y_2|]), \tag{3.10}$$

which will be used in Section 5.

4 A discrete Galerkin method for (DP)

In this section, we discuss the computation of synthetic near-field data $u(x_1,b)$ for an incident pressure wave by solving a first kind integral equation and using the discrete Galerkin method proposed by Atkinson [7]. The theoretical justification of this method is based on the decomposition (3.7) of $\Pi(x,y)$ and the periodicity of the grating surface. A similar method is used in [22] for solving the forward problem of elastic scattering from an open arc in $\mathbb{R}^2$. From the numerical view point, the implementation of this method is easier than in the case of the integral equation method with a second kind integral equation that involves the computation of the stress operator on the profile.

In the following subsections 4.1 and 4.2 we assume that Λ is the graph of some C^2-smooth periodic function f.

4.1 A first kind integral equation

We make the ansatz for the scattered field u in the form

$$u(x) = \int_\Lambda \Pi(x,y)\ \phi(y) ds(y), \quad x\in\Omega_\Lambda \tag{4.11}$$

with some unknown α-quasiperiodic function $\phi(y)\in L^2(\Lambda)^2$. Then we only need to solve the first kind linear integral equation

$$\int_\Lambda \Pi(x,y)\ \phi(y) ds(y) = -u^{in}(x) \qquad x\in\Lambda. \tag{4.12}$$

Set

$$x=(t,f(t)),\ y=(s,f(s)),\ g(t) := -u^{in}(t,f(t))\exp(-i\alpha t),$$
$$\rho(s) := \phi(s,f(s))\exp(-i\alpha s)\sqrt{1+f'(s)^2},\ K(t,s)=\Pi(t,f(t);s,f(s))\exp(i\alpha(s-t)).$$

Multiplying (4.12) by $\exp(-i\alpha t)$ gives the equivalent form

$$\int_0^{2\pi} K(t,s)\rho(s)ds = g(t), \quad 0\le t\le 2\pi. \tag{4.13}$$

Note that $\rho(t), g(t)$ are both 2π-periodic with respect to t. It follows from the second decomposition in (3.7) that

$$\begin{aligned} K(t,s) &= \left\{ -\eta_1 \frac{1}{\pi} \ln(\sqrt{(t-s)^2 + (f(t)-f(s))^2})\ I + \Pi^*(t, f(t); s, f(s)) \right\} \exp(i\alpha(s-t)) \\ &= -\eta_1 \frac{1}{\pi} \ln|2e^{-1/2} \sin(\frac{t-s}{2})|\ I + H(t,s), \end{aligned}$$

where

$$\begin{aligned} H(t,s) &:= K(t,s) + \eta_1 \frac{1}{\pi} \ln|2e^{-1/2} \sin(\frac{t-s}{2})|\ I \\ &= \left\{ -\eta_1 \frac{1}{\pi} \ln(\frac{\sqrt{(t-s)^2 + (f(t)-f(s))^2}}{2e^{-1/2}\sin((t-s)/2)})\ I + \Pi^*(t, f(t); s, f(s)) \right\} \exp(i\alpha(s-t)) \\ &\quad -\eta_1 \frac{1}{\pi} \ln|2e^{-1/2} \sin(\frac{t-s}{2})|(\exp(i\alpha(s-t)) - 1)\ I. \end{aligned}$$

Using the power series of the exponential function, we see that $H(t,s)$ is a continuously differentiable function on $\mathbb{R} \times \mathbb{R}$. Define the integral operators

$$A\rho(t) := -\eta_1 \frac{1}{\pi} \int_0^{2\pi} \ln|2e^{-1/2} \sin(\frac{t-s}{2})|\ I\rho(s)ds, \quad B\rho(t) := \int_0^{2\pi} H(t,s)\ \rho(s)ds. \tag{4.14}$$

It is seen from the periodicity of $\Pi(t, f(t); s, f(s)) \exp(i\alpha(s-t))$ and the kernel of A that the kernel $H(t,s)$ of B is 2π-periodic in both s and t. Let $H_p^1(0, 2\pi)$ denote the Sobolev space of 2π-periodic functions on $(0, 2\pi)$. Then, solving the first kind integral equation (4.13) can be transformed into:

$$\text{Given } g \in H_p^1(0,2\pi)^2, \text{ find } \rho(t) \in L^2(0,2\pi)^2 \text{ such that } A\rho + B\rho = g. \tag{4.15}$$

Lemma 4.1. *Problem (4.15) is always uniquely solvable.*

Proof. Since we have (see [7])

$$A(Ie^{imt}) = \frac{1}{\max\{1, |m|\}} Ie^{imt}, \quad m \in \mathbb{Z},$$

the operator $A : L^2(0,2\pi)^2 \to H_p^1(0,2\pi)^2$ is bounded and has a bounded inverse $A^{-1} : H_p^1(0,2\pi)^2 \to L^2(0,2\pi)^2$. The operator B is obviously compact from $L^2(0,2\pi)^2$ to $H_p^1(0,2\pi)^2$, since the kernel of B is continuously differentiable. Thus it suffices to consider the second kind equation $(I + A^{-1}B)\rho = A^{-1}g$. It follows from the uniqueness to the Dirichlet problem [13] combined with the jump relations for the periodic single-layer potential (see e.g. [2, 24] and the references therein) that the solution to the problem (4.15) is unique. Applying the Fredholm alternative yields the existence. □

4.2 The discrete Galerkin method for smooth gratings

Let $\mathcal{J}_n$ denote the $(2n+1)$-dimensional space of all trigonometric polynomials of degree not greater than n, with a basis given by $\{\varphi_m(t) := e^{imt}, \quad m = -n, -n+1, \cdots, 0, \cdots, n-1, n\}$. Let P_n denote

the orthogonal projection of $L^2(0,2\pi)^2$ onto $\mathcal{J}_n^2$ defined by

$$(P_n\rho)(t) = \frac{1}{\sqrt{2\pi}} \sum_{m=-n}^{n} \rho_m e^{imt}, \quad \rho_m = \frac{1}{\sqrt{2\pi}} \int_0^{2\pi} \rho(s) e^{-ims} ds \in \mathbb{C}^2.$$

The Galerkin method for (4.15) consists of solving

$$(A + P_n B)\rho_n = P_n g, \quad \text{for } \rho_n = \sum_{j=-n}^{n} c_j \varphi_j(t) \in \mathcal{J}_n^2, \quad c_j \in \mathbb{C}^2. \tag{4.16}$$

Let $C_p[0,2\pi]$ denote the continuous complex-valued 2π-periodic functions in t. The basic idea of the discrete Galerkin method proposed in [7] is to approximate the orthogonal projection P_n by the interpolatory projection $Q_n : C_p[0,2\pi]^2 \to \mathcal{J}_n^2$ at the equidistant grid points $t_j = jh, h = 2\pi/(2n+1)$, i.e., to approximate the Galerkin method (4.16) by

$$(A + Q_n B_n)\rho_n = Q_n g, \quad \rho_n \in \mathcal{J}_n^2, \tag{4.17}$$

where the integral operator B is approximated by a finite dimensional operator using the trapezoidal rule

$$B_n\rho_n(t) \;\; = \;\; h \sum_{j=0}^{2n} H(t,t_j)\rho_n(t_j). \tag{4.18}$$

To avoid the computation of $H(t,s)$ for $t = s$ (i.e. the diagonal terms), we introduce the collocation points $s_k = kh + h/2, k = 0,1,\cdots,2n$, which is a shift of the equidistant grid points t_j. Then, problem (4.17)-(4.18) is equivalent to

$$\sum_{j=-n}^{n} \left[\frac{\eta_1 \varphi_j(s_k)}{\max\{1,|j|\}} I + B_n \varphi_j(s_k) \right] c_j = g(s_k), \quad k = 0,1,\cdots,2n.$$

Using (4.18) and the orthogonality of φ_m, the previous finite linear system becomes (see also [17, section 3])

$$\sum_{j=0}^{2n} \left[\eta_1 \sigma_{kj} + hH(s_k,t_j) \right] \rho_n(t_j) = g(s_k), \quad k = 0,1,\cdots,2n, \tag{4.19}$$

in terms of the unknown density ρ, where

$$\sigma_{kj} = \frac{1}{2\pi} h \sum_{m=-n}^{n} \varphi_m(s_k)\overline{\varphi_j(t_m)} / \max\{1,|m|\}.$$

Note that $s_k \neq t_j$ for all $k,j = 0,1,\cdots,2n$, and that σ_{kj} can be readily obtained employing the fast Fourier transform.

4.3 The discrete Galerkin method for piecewise linear gratings

To apply the method in Section 4.2 to piecewise linear gratings where the scattered field may be singular at corner points, we adopt a mesh grading transformation (see e.g. [17]) to parameterize the grating profile. In this subsection the grating profile is assumed to be the graph of a piecewise linear function

$$f(x_1) = f(\xi_j) + \frac{f(\xi_{j+1}) - f(\xi_j)}{\xi_{j+1} - \xi_j}(x_1 - \xi_j), \quad \xi_j \le x_1 \le \xi_{j+1}, \quad j = 0,1,2,\cdots,r, \tag{4.20}$$

with $0 = \xi_0 < \xi_1 < \xi_2 < \cdots < \xi_r = 2\pi$. One can easily carry over the subsequent argument to the case of binary gratings.

Denote by Γ_j the line segment connecting $(\xi_j, f(\xi_j))$ and $(\xi_{j+1}, f(\xi_{j+1}))$, $j = 0, 1, \cdots, r-1$, and denote by $|\Gamma_j|$ the length of Γ_j. Choose a grading exponent $q \in \mathbb{N}$ and introduce the r points $0 = S_0 < S_1 < \cdots < S_{r-1} < S_r = 2\pi$ given by

$$(S_{j+1} - S_j)/2\pi = |\Gamma_j|^{1/q} / \sum_{j=0}^{r-1} |\Gamma_j|^{1/q}, \quad j = 0, \cdots, r-1.$$

Define the functions $\nu(s), \sigma_j(s)$ by

$$\begin{aligned} \nu(s) &= \begin{cases} s, \quad \text{if} \quad q = 1, \\ (1/q - 1/2)(1-2s)^3 + (1/q)(2s-1) + 1/2, \quad \text{if} \quad q \geq 2, \end{cases} \\ \sigma_j(s) &= \nu^q(\frac{s - S_j}{S_{j+1} - S_j}) \left\{ \nu^q(\frac{s - S_j}{S_{j+1} - S_j}) + \nu^q(\frac{S_{j+1} - s}{S_{j+1} - S_j}) \right\}^{-1}, \quad S_j \leq s \leq S_{j+1}, \end{aligned}$$

respectively, and define a new parameterization $\psi(s)$ of the grating profile Λ by

$$\psi(s) = \begin{pmatrix} \psi_1(s) \\ \psi_2(s) \end{pmatrix} := \begin{pmatrix} \xi_j \\ f(\xi_j) \end{pmatrix} + \sigma_j(s) \begin{pmatrix} \xi_{j+1} - \xi_j \\ f(\xi_{j+1}) - f(\xi_j) \end{pmatrix}$$

for $S_j \leq s \leq S_{j+1}, j = 0, \cdots, r-1$. Via this mesh grading transformation $\psi(s)$, one half of the grid points $\{\psi(s_k)\}$ is equally distributed over the grating profile, whereas the other half is accumulated towards the corner points. Multiplying the first kind integral equation (4.12) by $\exp(-i\alpha x_1)$ gives the equivalent form

$$\int_\Lambda \Pi(x, y) \exp(i\alpha(y_1 - x_1)) \tilde{\psi}(y) ds(y) = -u^{in}(x) \exp(-i\alpha x_1), \quad x \in \Lambda, \tag{4.21}$$

where $\tilde{\psi}(y) = \phi(y) \exp(-i\alpha y_1)$. Using the change of variables $x = (\psi_1(t), \psi_2(t)), y = (\psi_1(s), \psi_2(s))$, the equation (4.21) becomes

$$A\rho(t) + B\rho(t) := -\eta_1 \frac{1}{\pi} \int_0^{2\pi} \ln |2e^{-1/2} \sin(\frac{t-s}{2})| I\, \rho(s) ds + \int_0^{2\pi} H(t, s) \rho(s) ds = g(t), \tag{4.22}$$

where

$$\begin{aligned} &\rho(s) = |\psi'(s)| \tilde{\psi}(\psi_1(s), \psi_2(s)) \exp(-i\alpha(\psi_1(s)), \quad g(t) = -u^{in}(\psi_1(t), \psi_2(t)) \exp(-i\alpha\psi_1(t)), \\ &H(t, s) = \Pi(\psi_1(t), \psi_2(t); \psi_1(s), \psi_2(s)) \exp(i\alpha(\psi_1(s) - \psi_1(t))) + (\eta_1/\pi) \ln |2e^{-1/2} \sin(\tfrac{t-s}{2})|. \end{aligned}$$

Then, recalling the equidistant mesh $\{t_j\}$ and the collocation points $\{s_k\}$ defined in Section 4.2, we can compute the values $\rho(t_j)$ of the solution to the equation (4.22) by solving the finite linear system (4.19) with $g(t), H(t, s)$ given above; note that problem (4.22) takes the same form as (4.14)-(4.15). Finally, multiplying (4.11) by $\exp(-i\alpha x_1)$ and using the change of variable $y = (\psi_1(s), \psi_2(s))$, we obtain the near-field data $\exp(-i\alpha t) u(t, b)$ by

$$u(t, b) e^{-i\alpha t} = \int_0^{2\pi} \Pi(t, b; \psi_1(s), \psi_2(s)) \exp(i\alpha(\psi_1(s) - t))\ \rho(s) ds. \tag{4.23}$$

4.4 Formulas on computing the kernel H and the Rayleigh coefficients.

To solve (4.19), one needs to calculate the kernel $H(t,s)$ for $t \neq s$, where the values of $\exp(i\alpha(y_1 - x_1))\Pi(x,y)$ for $x - y \neq n(2\pi, 0), n \in \mathbb{Z}$, are required. Multiplying the representation (3.6) of the fundamental solution $\Pi(x,y)$ by $\exp(i\alpha(y_1 - x_1))$, we observe that the second part of $\exp(i\alpha(y_1 - x_1))\Pi(x,y)$ can be approximated by the difference of the finite series

$$\frac{i}{\omega^2 4\pi} \quad \Big\{ \sum_{|n|\le M} \frac{1}{\beta_n} \begin{pmatrix} \alpha_n^2 & \alpha_n\beta_n \mathsf{sign}(x_2 - y_2) \\ \alpha_n\beta_n \mathsf{sign}(x_2 - y_2) & \beta_n^2 \end{pmatrix} e^{in(x_1-y_1)+i\beta_n|x_2-y_2|} \\ - \sum_{|n|\le M} \frac{1}{\gamma_n} \begin{pmatrix} \alpha_n^2 & \alpha_n\gamma_n \mathsf{sign}(x_2 - y_2) \\ \alpha_n\gamma_n \mathsf{sign}(x_2 - y_2) & \gamma_n^2 \end{pmatrix} e^{in(x_1-y_1)+i\gamma_n|x_2-y_2|} \Big\}$$

for some integer $M > 0$, while the calculation of the first part concerning $G_{k_s}(x,y)e^{i\alpha(y_1-x_1)}$ can be accelerated by Ewald's method (see e.g. [23]). Consider the exponential integral function E_j of degree j and the scaled complementary error function σ defined by

$$E_j(z) = \int_1^\infty \frac{e^{-zt}}{t^j} dt, \quad \sigma(z) = e^{-z^2}\mathsf{erfc}(-iz) = \frac{2}{\sqrt{\pi}} \int_0^\infty e^{-t^2} e^{2izt} dt$$

respectively, where $\mathrm{erfc}(z)$ denotes the complementary error function. Then we have (see [24])

$$\exp(i\alpha(y_1 - x_1))G_{k_s}(x,y) = G_{k_s}^{(1)}(x,y) + G_{k_s}^{(2)}(x,y), \tag{4.24}$$

where, for any fixed $a > 0$,

$$G_{k_s}^{(1)}(x,y) = \tfrac{e^{-i\alpha(x_1-y_1)}}{4\pi} \textstyle\sum_{m\in\mathbb{Z}} e^{i2\pi m\alpha} \sum_{j=0}^\infty \frac{(ak_s)^{2j}}{j!} E_{j+1}\big(\frac{(x_1-y_1-2m\pi)^2+(x_2-y_2)^2}{4a^2}\big),$$
$$G_{k_s}^{(2)}(x,y) = \tfrac{ie^{-(x_2-y_2)^2/4a^2} e^{a^2k_s^2}}{8\pi} \textstyle\sum_{n\in\mathbb{Z}} \frac{e^{in(x_1-y_1)}e^{-a^2\alpha_n^2}}{\gamma_n} \left(\sigma(a\gamma_n + i\frac{x_2-y_2}{2a}) + \sigma(a\gamma_n - i\frac{x_2-y_2}{2a})\right).$$

Note that the formula (4.24) differs from that in [23], and it is efficient for binary grating diffraction problems where the values of $x_2 - y_2$ may be zero.

Given the solution ρ to (4.19), we may compute the near-field data $\exp(-i\alpha t)u(t,b)$ by

$$u_b^{(p)}(t) := u(t,b)e^{-i\alpha t} = \int_0^{2\pi} \Pi(t,b;s,f(s)) \exp(i\alpha(s-t))\rho(s)ds, \ \rho = (\rho_1,\rho_2)^T, \tag{4.25}$$

for a smooth grating profile. However, since our reconstruction method in Section 5 only requires the knowledge of the Rayleigh coefficients $A_{p,n}$ and $A_{s,n}$, we will calculate these coefficients from ρ directly in order to avoid computing $\Pi(t,b;s,f(s))\exp(i\alpha(s-t))$ in (4.25). Let

$$u^{(p)}(x) := e^{-i\alpha x_1}u(x) = \sum_{n\in\mathbb{Z}} A_{p,n} \begin{pmatrix} \alpha_n \\ \beta_n \end{pmatrix} e^{inx_1+i\beta_n x_2} + A_{s,n} \begin{pmatrix} -\gamma_n \\ \alpha_n \end{pmatrix} e^{inx_1+i\gamma_n x_2} \tag{4.26}$$

for $x_2 > \Lambda_f^+$. It follows from (3.8)-(3.10) and (4.25) that the compressional part $u_p^{(p)}$ of $u^{(p)}$ is given by

$$u_p^{(p)}(x) \quad = \quad \frac{i}{\omega^2 4\pi} \sum_{n\in\mathbb{Z}} \left\{ \frac{1}{\beta_n} \begin{pmatrix} \alpha_n^2 & \alpha_n\beta_n \\ \alpha_n\beta_n & \beta_n^2 \end{pmatrix} e^{inx_1+i\beta_n x_2} \int_0^{2\pi} e^{-ins-i\beta_n f(s)} \rho(s) ds \right\},$$

from which we can derive the Rayleigh coefficients $A_{p,n}$ as

$$A_{p,n} = \frac{i}{\omega^2 4\pi\beta_n}\left\{\int_0^{2\pi} e^{-ins-i\beta_n f(s)}(\alpha_n\rho_1(s)+\beta_n\rho_2(s))ds\right\}, \quad n\in\mathbb{Z}.$$

Analogously, the shear part $u_s^{(p)}(x)$ of $u^{(p)}(x)$ is given by

$$\begin{aligned} u_s^{(p)}(x) &= \frac{i}{4\pi}\sum_{n\in\mathbb{Z}}\left\{\frac{1}{\gamma_n\mu}I-\frac{1}{\gamma_n\omega^2}\begin{pmatrix}\alpha_n^2 & \alpha_n\gamma_n\\ \alpha_n\gamma_n & \beta_n^2\end{pmatrix}\right\}e^{inx_1+i\gamma_n x_2}\int_0^{2\pi} e^{-ins-i\gamma_n f(s)}\rho(s)ds \\ &= \frac{i}{4\pi\omega^2}\sum_{n\in\mathbb{N}}\frac{1}{\gamma_n}\begin{pmatrix}\gamma_n^2 & -\alpha_n\gamma_n\\ -\alpha_n\gamma_n & \alpha_n^2\end{pmatrix}e^{inx_1+i\gamma_n x_2}\int_0^{2\pi} e^{-ins-i\gamma_n f(s)}\rho(s)ds, \end{aligned}$$

which together with (4.25) and (4.26) leads to

$$A_{s,n} = \frac{i}{\omega^2 4\pi\gamma_n}\left\{\int_0^{2\pi} e^{-ins-i\gamma_n f(s)}(\alpha_n\rho_2(s)-\gamma_n\rho_1(s))ds\right\}, \quad n\in\mathbb{Z}.$$

The above argument on computing the Rayleigh coefficients for a smooth grating profile can be easily extended to the case of a piecewise linear grating; cf. (4.25) and (4.23).

Given some $b>\Lambda^+$, we can now rewrite the near-field data $u_b(x_1)=u(x_1,b)$ as

$$u_b(x_1)=\sum_{n\in\mathbb{Z}}\mathbf{A}_n(\theta)\exp(i\alpha_n x_1),\ \mathbf{A}_n(\theta):=A_{p,n}(\alpha_n,\beta_n)^T e^{i\beta_n b}+A_{s,n}(-\gamma_n,\alpha_n)^T e^{i\gamma_n b}, \quad (4.27)$$

and analogously represent the far-field data $u_b^\infty(x_1)$ as

$$u_b^\infty(x_1)=\sum_{n\in\mathcal{U}_s}\mathbf{A}_n^\infty(\theta)\exp(i\alpha_n x_1),$$

where

$$\mathbf{A}_n^\infty(\theta)=\begin{cases} A_{p,n}(\alpha_n,\beta_n)^T e^{i\beta_n b}+A_{s,n}(-\gamma_n,\alpha_n)^T e^{i\gamma_n b}, & \text{if } n\in\mathcal{U}_p,\\ A_{p,n}(\alpha_n,\beta_n)^T e^{i\beta_n b}, & \text{if } n\in\mathcal{U}_s\backslash\mathcal{U}_p.\end{cases} \quad (4.28)$$

5 A two-step algorithm for (IP)

In our numerical examples we mainly consider the following equivalent problem to (**IP**):

(**IP'**): Given an incident plane pressure wave $u^{in}(x;\theta)$ and the coefficients $\mathbf{A}_n(\theta), n\in\mathbb{Z}$ defined in (4.27) for some $b>\Lambda^+$, determine the unknown grating profile Λ lying between the straight lines $\{x_2=0\}$ and $\{x_2=b\}$.

Consider the Hilbert space $X=L^2(0,2\pi)^2$ with the scalar product

$$(x(t),y(t))=\frac{1}{2\pi}\int_0^{2\pi} x(t)\cdot\overline{y(t)}dt,$$

and the norm $||x|| := \sqrt{(x,x)}$. For $a = (a_1, a_2) \in \mathbb{C}^2$, define $|a| = \sqrt{|a_1|^2 + |a_2|^2}$. Given $\varphi \in X$, define the linear operators $T, S_f : X \to X$ by

$$T\varphi(x_1) = \frac{1}{2\pi} \int_0^{2\pi} \Pi(x_1, b; t, 0)\varphi(t)dt, \quad S_f\varphi(x_1) = \frac{1}{2\pi} \int_0^{2\pi} \Pi(x_1, f(x_1); t, 0)\varphi(t)dt.$$

The Kirsch-Kress method adapted to our diffraction problem consists of solving the following optimization problem

$$||T\varphi - u_b||^2 + \gamma||\varphi||^2 + \eta||u^{in} \circ f + S_f\varphi||^2 \to \inf_{f \in \mathcal{M}, \varphi \in X}, \tag{5.29}$$

where $\gamma > 0$ denotes the regularization parameter, $\eta > 0$ is a coupling parameter and $\mathcal{M}$ is an admissible set of profile functions with uniformly bounded $C^{0,1}$-norm. Here and in the following we identify the (α-quasiperiodic) space $L^2(\Lambda_f)^2$ with X via $v \to v \circ f$:

$$v \circ f = v(t, f(t)), \quad t \in [0, 2\pi],$$

such that

$$||v \circ f||_X = \left(\frac{1}{2\pi} \int_0^{2\pi} |v(t, f(t))|^2 dt \right)^{1/2}, \quad v \in L^2(\Lambda)^2,$$

is a uniformly equivalent norm in $f \in \mathcal{M}$. The convergence analysis for problem (5.29) is presented in [18] in the case of the quasiperiodic Helmholtz equation, which we think can carry over to the quasiperiodic Navier equation. Since the combined optimization scheme (5.29) requires the determination of two unknown functions f and φ, to reduce computational efforts we apply the two-step inversion algorithm of [18] to the inverse elastic scattering problem (**IP'**). It is shown in [18] that this algorithm is faster and gives similar or more accurate results than for the combined algorithm based on the minimization of (5.29). However, the convergence of the two-step algorithm is still open.

5.1 First step: reconstruct the scattered field from near-field data

We suppose that the scattered field $u(x)$ can be represented as a single layer potential

$$u(x) = \int_0^{2\pi} \Pi(x_1, x_2; t, 0)\varphi(t)dt, \quad x \in \Omega_\Lambda$$

with some unknown α-quasi-periodic function $\varphi(t) \in X$. Then, it suffices to solve the first kind integral equation

$$T\varphi(x_1) = u_b(x_1) \quad \text{for all} \quad x_1 \in (0, 2\pi),$$

which is linear but severely ill-posed. We expand $\varphi(t) \in X$ into the series

$$\varphi(t) = \sum_{n \in \mathbb{Z}} \varphi_n \exp(i\alpha_n t), \quad \varphi_n := (\varphi_n^{(1)}, \varphi_n^{(2)}) \in \mathbb{C}^2. \tag{5.30}$$

It follows from (3.8)-(3.10) that

$$\begin{aligned} T\varphi(x_1) &= \frac{1}{2\pi}\int_0^{2\pi} \Pi(x_1, b; t, 0)\varphi(t)dt \\ &= \sum_{n\in\mathbb{Z}} \left\{ P^{(n)}\varphi_n \exp(i[\alpha_n x_1 + \beta_n b]) + S^{(n)}\varphi_n \exp(i[\alpha_n x_1 + \gamma_n b]) \right\} \\ &= \sum_{n\in\mathbb{Z}} M^{(n)}\varphi_n \exp(i\alpha_n x_1), \end{aligned}$$

where $M^{(n)}$ is the 2×2 matrix given by

$$M^{(n)} := \left(P^{(n)} \exp(i\beta_n b) + S^{(n)} \exp(i\gamma_n b) \right).$$

Instead of solving $T\varphi = u_b$, we consider the Tikhonov regularized version

$$\gamma\varphi + T^*T\varphi = T^*u_b \tag{5.31}$$

with the regularization parameter $\gamma > 0$, where T^* denotes the adjoint operator of T. Let the singular value decomposition of $M^{(n)}$ be given by

$$M^{(n)} = U^{(n)}\,\Sigma^{(n)}\,(V^{(n)})^*, \tag{5.32}$$

where

$$U^{(n)} = (U_1^{(n)}, U_2^{(n)}),\ V^{(n)} = (V_1^{(n)}, V_2^{(n)}),\ \Sigma^{(n)} = \mathsf{diag}(\sigma_1^{(n)}, \sigma_2^{(n)}).$$

with $U_j^{(n)}, V_j^{(n)} \in \mathbb{C}^2$ being column vectors and $\sigma_j^{(n)} \in \mathbb{R}^+$ for $n \in \mathbb{Z}$, $j = 1, 2$. Then, the set $\{V_j^{(n)} \exp(i\alpha_n t) : j = 1, 2, n \in \mathbb{Z}\}$ is an orthonormal basis of X. Thus the solution φ_γ to (5.31) is given by (see [12, Chapter 4])

$$\begin{aligned} \varphi_\gamma &= \sum_{n\in\mathbb{Z}}\sum_{j=1}^{2} \frac{\sigma_j^{(n)}}{(\sigma_j^{(n)})^2 + \gamma} \left(u_b, U_j^{(n)} \exp(i\alpha_n t) \right) V_j^{(n)} \exp(i\alpha_n t) \\ &\approx \sum_{|n|\le K}\sum_{j=1}^{2} \frac{\sigma_j^{(n)}}{(\sigma_j^{(n)})^2 + \gamma} (\mathbf{A}_n \cdot \overline{U_j^{(n)}})\, V_j^{(n)} \exp(i\alpha_n t) \end{aligned} \tag{5.33}$$

for some $K \in \mathbb{N}$, where $\mathbf{A}_n \in \mathbb{C}^2$ are defined in (4.27). Now we can represent φ_γ as

$$\varphi_\gamma = \sum_{|n|\le K} \varphi_\gamma^{(n)} \exp(i\alpha_n t), \quad \varphi_\gamma^{(n)} := \sum_{j=1}^{2} \frac{\sigma_j^{(n)}}{(\sigma_j^{(n)})^2 + \gamma} (\mathbf{A}_n \cdot \overline{U_j^{(n)}})\, V_j^{(n)}. \tag{5.34}$$

5.2 Second step: find the profile function by least squares minimization

Having computed φ_γ from the first step, we may consider $S_f(\varphi_\gamma)$ as an approximation of the values of the scattered field on the grating profile. Since the Dirichlet boundary condition is under consideration, we now turn to investigating the nonlinear least squares minimization problem

$$||u^{in} \circ f + S_f\varphi_\gamma|| \to \inf_{f\in\mathcal{M}}, \tag{5.35}$$

over some admissible set $\mathcal{M}$. Using (3.8)-(3.10) and (5.34), we see that

$$\begin{aligned} S_f\varphi_\gamma(x_1) &= \frac{1}{2\pi}\int_0^{2\pi} \Pi(x_1, f(x_1); t, 0)\varphi_\gamma(t)dt \\ &= \sum_{|n|\le K} P^{(n)}\varphi_\gamma^{(n)} \exp(i\alpha_n x_1 + i\beta_n f(x_1)) + S^{(n)}\varphi_\gamma^{(n)} \exp(i\alpha_n x_1 + i\gamma_n f(x_1)). \end{aligned}$$

Hence, the problem (5.35) is equivalent to

$$||\hat{\theta}e^{-i\beta f(t)} + \sum_{|n|\le K} \left(P^{(n)}\varphi_\gamma^{(n)} e^{i\beta_n f(t)} + S^{(n)}\varphi_\gamma^{(n)} e^{i\gamma_n f(t)}\right) e^{int}||^2 \to \inf_{f\in\mathcal{M}}. \tag{5.36}$$

In our numerical examples we discretize the objective functional in (5.36) by the trapezoidal rule and then solve the resulting minimization problem in a finite dimensional space.

Case 1: Λ is a C^2-smooth grating profile.

We define the admissible set $\mathcal{M}$ as

$$\mathcal{M} = \left\{ f(t) = a_0 + \sum_{m=1}^{M} a_m \cos(mt) + a_{M+m}\sin(mt) \right\} \tag{5.37}$$

for some fixed number $M \in \mathbb{N}$, where the Fourier coefficients $a_j, j = 0, 1, \cdots, 2M$ are supposed to be bounded. Then the left hand side of (5.36) can be approximated by

$$F(\mathbf{a}, \theta) \approx \frac{1}{2\pi}\sum_{j=1}^{N} F_j(\mathbf{a}, \theta), \quad \mathbf{a} = (a_0, \cdots, a_{2M}) \in \mathbb{R}^{2M+1} \tag{5.38}$$

for some $N \in \mathbb{N}$, where

$$F_j(\mathbf{a}, \theta) = \frac{1}{N}|\hat{\theta}e^{-i\beta f(s_j)} + \sum_{|n|\le K} \left(P^{(n)}\varphi_\gamma^{(n)} e^{i\beta_n f(s_j)} + S^{(n)}\varphi_\gamma^{(n)} e^{i\gamma_n f(s_j)}\right) e^{ins_j}|^2$$

with $s_j = 2\pi(j-1)/N, j = 1, 2, \cdots, N$. Note that the values of $f(s_j)$ depend on **a**.

Case 2: Λ is a piecewise linear grating profile.

Consider the piecewise linear grating (4.20) with the parameters $\xi_j, d_j := f(\xi_j)$ satisfying

$$0 = \xi_0 < \xi_1 < \cdots < \xi_r = 2\pi, \quad d_j > 0, \quad j = 0, 1, \cdots, r, \quad d_0 = d_r$$

for some fixed number $r \in \mathbb{N}$. We assume that the the parameters d_j are uniformly bounded and that the minimal distance between partition points ξ_j remains uniformly bounded from below. This allows us to define the admissible class $\mathcal{M}$ by

$$\mathcal{M} = \{f(t) = \xi_j + T_j\ (t - \xi_j), \quad t \in [\xi_j, \xi_{j+1}],\ j = 0, 1, \cdots, r-1\}$$

with $T_j := (d_{j+1} - d_j)/(\xi_{j+1} - \xi_j)$. Then we approximate the left hand side of (5.36) by

$$F(\mathbf{a}, \theta) \approx \frac{1}{2\pi}\sum_{j=0}^{r-1} F_j(\mathbf{a}, \theta), \quad \mathbf{a} = (\xi_1, \cdots, \xi_{r-1}, d_0, d_1 \cdots, d_{r-1}) \in \mathbb{R}^{2r-1} \tag{5.39}$$

where

$$F_j(\mathbf{a},\theta)=\int_{t_j}^{t_{j+1}}|\hat{\theta}e^{-i\beta f(s)}+\sum_{|n|\le K}\left(P^{(n)}\varphi_\gamma^{(n)}e^{i\beta_n f(s)}+S^{(n)}\varphi_\gamma^{(n)}e^{i\gamma_n f(s)}\right)e^{ins}|^2\,ds$$

for $j=0,1,\cdots,r-1$. In our numerical examples we consider a linear l-tower grating profile where $r=4\,l$ for some $l\in\mathbb{N}$ and

$$f(t_j)=\begin{cases} d_0>0, & \text{for} \quad j=4n,4n+1,\\ d_1>0, & \text{for} \quad j=4n+2,4n+3,\end{cases}\qquad n=0,1,\cdots,l.$$

In this special case, only a $(r+1)$-dimensional vector $\mathbf{a}=(\xi_1,\cdots,\xi_{r-1},d_0,d_1)$ needs to be updated.

We finally note that the finite dimensional least squares problems (5.38) and (5.39) can be solved using the Gauss-Newton or Levenberg-Marquardt method (see [9] for the Helmholtz equation). In our experiments we set lower and upper bounds on the unknown parameter **a** and employ the subroutine *lsqnonlin* from the Optimization Tool Box of MATLAB for solving the minimization problem by the Trust-Region Reflective algorithm. We note that the singular value decomposition in (5.32) can be easily achieved by using the subroutine *svd*, and we can observe that $\sigma_j^{(n)}\to 0$, $j=1,2$ as $n\to+\infty$ so that the integral operator T is indeed compact.

Remark 5.1. *(i) The method in case 2 can be applied to binary gratings. We refer to [9] for the reconstruction of such gratings, where only the Dirichlet data on the horizontal line segments are involved in the computation. Note that a binary grating profile is not the graph of a continuous function. In our experiments the Dirichlet data on the whole binary grating profile are used.*

*(ii) Consider the profile reconstruction problem (**IP***) using the far-field data $u_b^\infty(x_1,\theta_\tau)$ for several incoming waves with different incident angles $\theta_\tau\in(-\pi/2,\pi/2),\tau=1,2,\cdots,m$. In this case, the Tikhonov regularized solution to the equation $T\varphi=u_b^\infty$ is given by*

$$\varphi_\gamma(\theta_\tau)=\sum_{n\in\mathcal{U}_s}\varphi_\gamma^{(n)}\exp(i\alpha_n t),\quad \varphi_\gamma^{(n)}:=\sum_{j=1}^{2}\frac{\sigma_j^{(n)}}{(\sigma_j^{(n)})^2+\gamma}(\boldsymbol{A}_n^\infty(\theta_\tau)\cdot\overline{U_j^{(n)}})\,V_j^{(n)},$$

where the coefficients $\boldsymbol{A}_n^\infty(\theta_\tau),n\in\mathcal{U}_s$ are defined in (4.28). Denote by $F(\mathbf{a},\theta_\tau)$ the objective functional in (5.39) corresponding to the incident field $u^{in}(x;\theta_\tau)$. Then we only need to perform computations with the cost function

$$\mathcal{F}(\mathbf{a})=\sum_{\tau=1}^{m}F(\mathbf{a},\theta_\tau).$$

6 Numerical examples

Here we present the results of numerical experiments using our method with exact and noisy data. Unless otherwise stated, we always assume that $k_s=4.45$, $\omega=5$, and probe the unknown grating profile by a single incident pressure wave with $\theta=0$ and $k_p=4.2$. With these settings we have

$$\mathcal{U}_p=\mathcal{U}_s=\{n\in\mathbb{Z}:|n|\le 4\}.$$

The exact values of the coefficients $\mathbf{A}_n$ in (4.27) are produced using the discrete Galerkin method described in Section 4. To generate noisy data with noise level $\delta \geq 0$, we first perturb the exact near-field data $u_b^{(p)}$ in (4.25) with the following random errors

$$u_{b,\delta}^p(t_j) := u_b^{(p)}(t_j) + \delta \; u_b^{(p)}(t_j) \; \omega_j,$$

where $\{t_j\}$ is the equidistant partition of $[0, 2\pi]$ given in Section 4.2 and ω_j are random values between -1 and 1, and then consider the Fourier coefficients $\mathbf{A}_n^\delta$ of $u_{b,\delta}^p$ as the noisy data of $\mathbf{A}_n$ with the noise level δ.

In the following examples 6.1 and 6.2, we set $K = 7$ (see (5.33)). This implies that all the propagating modes of the compressional and shear parts corresponding to $|n| \leq 4$ are used, while six additional evanescent modes corresponding to $5 \leq |n| \leq 7$ are also taken into account.

Example 6.1. Fourier gratings. Suppose that the grating profile function is given by a finite Fourier series

$$f(t) = 2 + \zeta(\cos(t) + \cos(2t) + \cos(3t)), \quad \zeta = 0.05\pi, \tag{6.40}$$

where ζ characterizes the steepness of the profile. We use both exact and noisy near-field data to reconstruct this profile function, which has the form (5.37) with $M = 3$. The computational results are given in table 1, where UB resp. LB denotes the upper resp. lower bounds imposed on the unknown vector $\mathbf{a} = \{a_0, \cdots, a_6\}$. The iteration is stopped when the changes of all elements in $\mathbf{a}$ (i.e. the termination tolerance on a_j) are less than 10^{-6}. Without the lower and upper bounds, the reconstruction becomes more sensitive to the initial guess and requires more iterations. If the initial value of a_0 is greater than 2.2, then the reconstruction fails. We select the regularization parameter γ by trial and error, and present the result in the case of $\gamma = 10^{-12}$ which is closest to the target among all our experiments. We observe that the computation would not be stationary if γ were less than 10^{-12}, and that (see table 1) noisy data even with noise level $\delta = 10\%$ can still produce good results. However, the results are not acceptable if we increase the steepness to 0.1π or only use the propagating modes.

Example 6.2. General C^2-smooth gratings. Suppose that Λ is the graph given by the function

$$f(t) = 1.5 + 0.2\exp(\sin(3t)) + 0.3\exp(\sin(3t)),$$

which can be approximated by a truncated Fourier series

$$f^*(t) = 2.133 - 0.0543\cos(6t) - 0.0814\cos(8t) + 0.22606\sin(3t) + 0.339\sin(4t).$$

In this case we choose $M = 8$ in (5.37) and still take the regularization parameter $\gamma = 10^{-12}$. The computational results are presented in table 2 and figure 1. Since the steepness of Λ is relatively large, the downward convex part of the grating surface is not well-reconstructed by our method. One can see that data with 10% noise lead to a larger deviation in contrast to the figure reconstructed from data corresponding to a noise of 5%.

Table 1: Example 6.1. $M = 3$, $\gamma = 10^{-12}$, $K = 7$, Ite=iterations.

	a_0	a_1	a_2	a_3	a_4	a_5	a_6	δ	Ite
Target	2	0.157	0.157	0.157	0	0	0		
Initial	0	0	0	0	0	0	0		
LB	-5	0	0	0	0	0	0		
UB	-5	0	0	0	0	0	0		
Computed	2.0026	0.1590	0.1610	0.1596	0	0	0	0	26
Computed	2.0029	0.1585	0.1592	0.1609	0.0004	0.0001	0.0001	0.05	25
Computed	2.0021	0.1594	0.1610	0.1595	0.0003	-0.0010	-0.0005	0.08	26
Computed	2.0029	0.1609	0.1601	0.1600	0.0023	-0.0019	0.0018	0.1	27

Example 6.3. Piecewise linear gratings. Consider a linear two-tower profile of height 1 above the straight line $x_2 = 2$ (i.e. $l = 2, r = 4$ in case 2 of Section 5). We perform numerical experiments by setting $K = 7, 4, 3$ respectively, with the final results given in table 3 and figure 2. Note that all far-field data are involved if $K = 4$, whereas only a part of the propagating modes are taken into account if $K = 3$. It is seen from table 2 that $K = 7$ and $K = 4$ can produce the same results, while $K = 3$ leads to an unsatisfactory reconstruction. Thus the knowledge of the Rayleigh coefficients for evanescent modes is necessary for an accurate recovery. We observe that the computational results in this case are very sensitive to the regularization parameter γ and the initial values of d_0 and d_1, but are less sensitive to the initial values of a_j, $j = 1, 2, \cdots, 7$. Choices of γ less or greater than 10^{-4} all lead to large deviations in the results. If the initial value of d_0 is less than 2.6 or that of d_1 is less than 1.7, the reconstruction fails. The number of total iterations needed is around 50.

Example 6.4. Binary gratings. Again we reconstruct a two-tower profile of height one over the level two. We use unperturbed far-field data (i.e. $K = 4$) from three incoming pressure waves for the three different incident angles $\theta = \pi/4, 0, \pi/4$ and a fixed compressional wave number $k_p = 4.2$. The results are given in table 4 and figure 3 (left). The reconstruction from the far-field data for a single incident angle $\theta = 0$ is also acceptable, but requires a better initial guess than in the case of three incident waves, see figure 3 (right). The reconstruction with three incoming waves appears to be more robust with respect to the initial values of t_1, t_2, t_3.

7 Conclusions

We adapt the two-step algorithm proposed by G. Bruckner and J. Elschner [9] to the more complicated case of elastic scattering for the reconstruction of one-dimensional grating profiles. In our reported examples, the near-field and far-field data are generated by a discrete Galerkin method, and the Tikhonov regularization is employed for both exact and noisy data with a regularization parameter selected by trial and error. We assume that *a prior* information on the smoothness of scattering surface (e.g. C^2-smooth

Table 2: Example 6.2. $M = 8, \gamma = 10^{-12}, K = 7$

	Target	Initial	LB	UB	Computed			
a_0	2.133	2.2	0	5	2.258	2.2256	2.2315	2.2900
a_1	0	0	0	1	0.1086	0.1078	0.1072	0.1124
a_2	0	0	0	1	0.0539	0.0534	0.0542	0.0112
a_3	0	0	0	1	0.0007	0.0018	0.0047	0.0136
a_4	0	0	0	1	0	0	0.0079	0.0212
a_5	0	0	0	1	0.05	0.0612	0.0567	0.0086
a_6	-0.0543	0	-2	1	0.0199	0.0195	-0.0319	0.0459
a_7	0	0	0	1	-0.0242	-0.0255	-0.0239	0.0044
a_8	-0.0814	0	-2	1	-0.0602	-0.0605	-0.0543	-0.0150
a_9	0	0	0	1	0.0204	-0.0198	-0.0001	0.0483
a_{10}	0	0	0	1	0	0	0	-0.0025
a_{11}	0	0	0	1	0.1371	0.1374	0.1322	0.0913
a_{12}	0.339	0	0	1	0.2469	0.2462	0.2514	0.2577
a_{13}	0	0	0	1	0	0	0	0.0299
a_{14}	0.22606	0	0	1	0.0423	0.0421	0.0253	0.0031
a_{15}	0	0	0	1	0.0070	0.0075	0.0087	-0.0085
a_{16}	0	0	0	1	0.0020	0.0028	0.0022	0.0201
δ					0	0.05	0.08	0.1
Ite					94	94	96	94

Table 3: Example 6.3. $\delta = 0, \gamma = 10^{-4}$.

	ξ_1	ξ_2	ξ_3	ξ_4	ξ_5	ξ_6	ξ_7	d_0	d_1	K
Target	0.5708	1.5708	2.1416	3.1416	3.7124	4.7124	5.2832	3	2	
Initial	0.0708	0.8208	1.6416	2.6416	3	4.2124	5.0332	2.6	1.7	
LB	0	0	0	0	0	0	π	2	1	
UB	2π	2π	2π	2π	2π	2π	2π	4	3	
Computed	0.7051	1.3901	2.0392	3.1507	3.8298	4.4273	5.0948	2.9536	2.0561	7
Computed	0.7051	1.3901	2.0392	3.1507	3.8298	4.4273	5.0948	2.9536	2.0561	4
Computed	0.4241	1.2902	1.8234	2.7713	3.3181	4.5001	5.0977	2.5291	1.8095	3

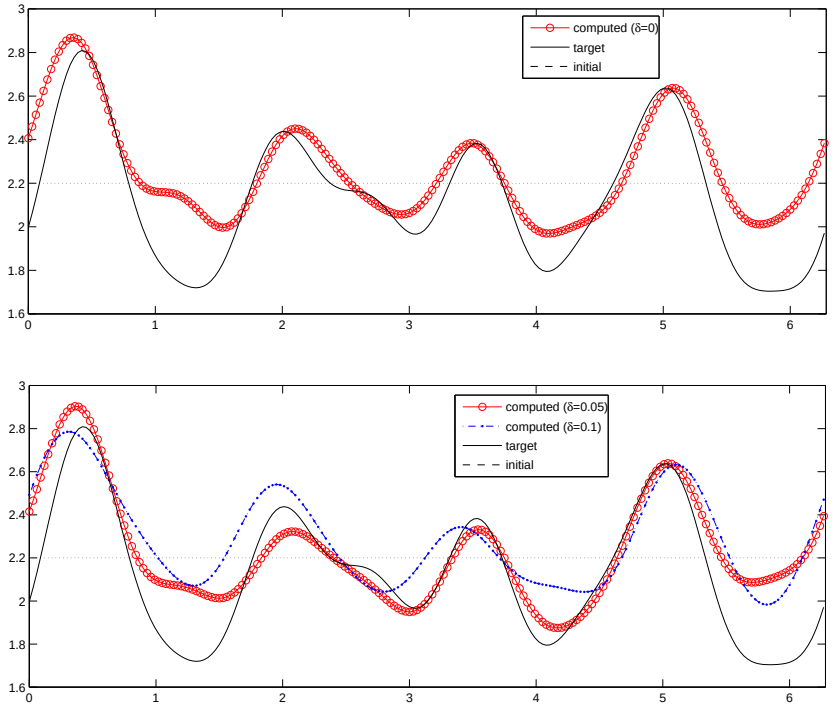

Figure 1: Example 6.2.

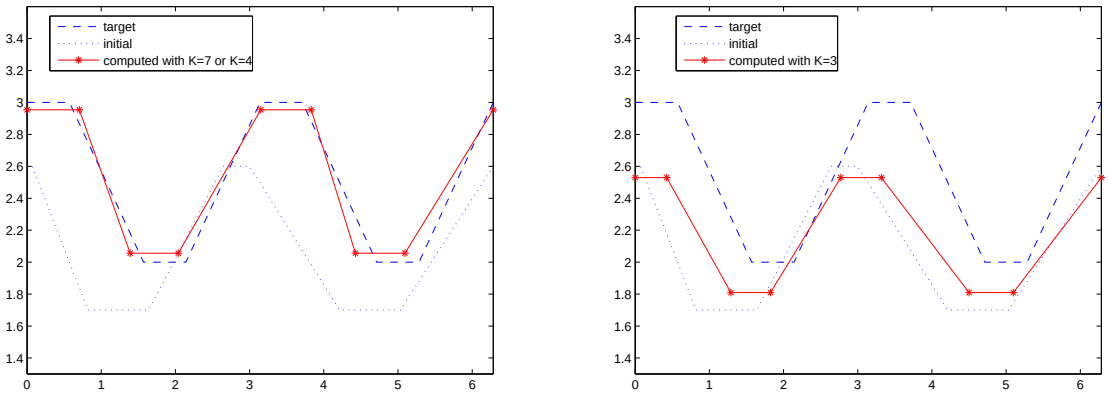

Figure 2: Example 6.3

Table 4: Example 6.4. $\delta = 0$, $\gamma = 10^{-4}$, $K = 4$.

	ξ_1	ξ_2	ξ_3	d_0	d_1
Target	1	3	5	3	2
Initial	0.4	1.8	5.8	2.6	1.7
LB	0	0	0	0	0
UB	2π	2π	2π	5	5
Computed	0.8629	3.1643	5.1041	2.9795	2.1086

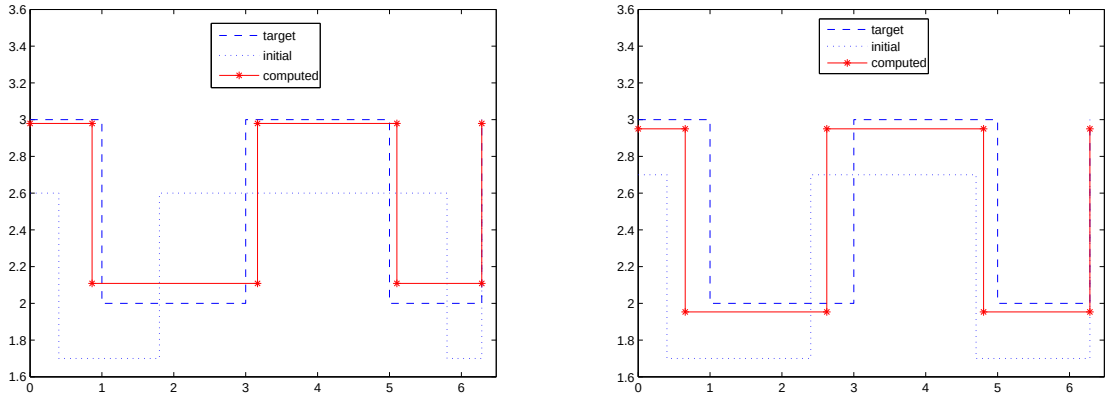

Figure 3: Example 6.4. Reconstruct a binary grating profile from the far-field data corresponding to three incident angles $\theta = -\pi/4, 0, \pi/4$ (left) or one single incident angle $\theta = 0$ (right).

or piecewise linear) is given, and that the unknown grating profile always has a finite number of parameters (e.g. Fourier coefficients or corner points) whose lower and upper bounds are known. Under such assumptions, the two-step algorithm is easily implemented and satisfactory reconstructions can be achieved with a low computational effort for suitable initial values. Our reconstruction scheme using far-field data for several incident angles can be readily extended to the case of a finite number of incident frequencies; note that in this paper we used a fixed compressional wave number $k_p = 4.2$. Since a larger compressional wave number leads to additional propagating modes, further work is still required to investigate the performance of the inversion algorithm depending on the wave number k_p and the parameter K in (5.33).

References

[1] Antonios C, Drossos G and Kiriakie K 2001 On the uniqueness of the inverse elastic scattering problem for periodic structures *Inverse Problems* **17** 1923–1935

[2] Arens T 1999 The scattering of plane elastic waves by a one-dimensional periodic surface *Math. Meth. Appl. Sci.* **22** 55–72

[3] Arens T 2001 Uniqueness for elastic wave scattering by rough surfaces *SIAM J.Math.Anal.* **33** 461–471

[4] Arens T 2002 Existence of solution in elastic wave scattering by unbounded rough surfaces *Math. Meth. Appl. Sci.* **25** 507–528

[5] Arens T and Grinberg N 2005 A complete factorization method for scattering by periodic surface *Computing* **75** 111-132

[6] Arens T and Kirsch A 2003 The factorization method in inverse scattering from periodic structures *Inverse Problems* **19** 1195-1211

[7] Atkinson K E 1988 A discrete Galerkin method for first kind integral equations with a logarithmic kernel *J. Integral Equations and Applications* **1** 343-363

[8] Bao G, Cowsar L and Masters W (eds.) 2001 *Mathematical Modeling in Optical Science* Philadelphia, USA: SIAM

[9] Bruckner G and Elschner J 2003 A two-step algorithm for the reconstruction of perfectly reflecting periodic profiles *Inverse Problems* **19** 315-329

[10] Bruckner G and Elschner J 2005 The numerical solution of an inverse periodic transmission problem *Math. Meth. Appl. Sci.* **28** 757-778

[11] Bruckner G, Elschner J and Yamamoto M 2003 An optimization method for profile reconstruction. In: *Progress in Analysis, Proceed. 3rd ISAAC congress* (Singapore: World Scientific) 1391-1404

[12] Colton D and Kress R 1998 *Inverse Acoustic and Electromagnetic Scattering Theory* 2nd Edition (Berlin: Springer)

[13] Elschner J and Hu G 2010 Variational approach to scattering of plane elastic waves by diffraction gratings *Math. Meth. Appl. Sci.* **33** 1924-1941 doi: 10.1002/mma.1305

[14] Elschner J and Hu G 2010 Inverse scattering of elastic waves by periodic structures: Uniqueness under the third or fourth kind boundary conditions *WIAS Preprint* No. **1528**

[15] Elschner J and Hu G 2010 Scattering of plane elastic waves by three-dimensional diffraction gratings *WIAS Preprint* No. **1565**

[16] Elschner J and Hu G 2011 Uniqueness in inverse scattering of elastic waves by three-dimensional polyhedral diffraction gratings *WIAS Preprint* No. **1591**

[17] Elschner J and Stephan E P 1996 A discrete collocation method for Symm's integral equation on curves with corners *Journal of Computational and Applied Mathematics* **75** 131-146

[18] Elschner J and Yamamoto M 2002 An inverse problem in periodic diffractive optics: reconstruction of Lipschitz grating profiles *Applicable Analysis* **81** 1307–1328

[19] Hettlich F 2002 Iterative regularization schemes in inverse scattering by periodic structures *Inverse Problems* **18** 701-714

[20] Hettlich F and Kirsch A 1997 Schiffer's theorem in inverse scattering for periodic structures *Inverse Problems* **13** 351-361

[21] Ito K and Reitich F 1999 A high-order perturbation approach to profile reconstruction: I. Perfectly conducting grating *Inverse Problems* **15** 1067-1085

[22] Kress R 1996 Inverse elastic scattering from a crack *Inverse Problems* **12** 667-684

[23] Linton C M 1998 The Green's function for the two-dimensional Helmholtz equation in periodic domains *Journal of Engineering Mathematics* **33** 377-401 DOI: 10.1023/A:1004377501747

[24] Rathsfeld A, Schmidt G and Kleemann B H 2006 On a fast integral equation method for diffraction gratings *Commun. Comput. Phys* **1** 984-1009

[25] Turunen J and Wyrowski F (eds) 1997 *Diffractive Optics for Industrial and Commercial Applications* (Berlin: Akademie)